

## Supporting Information to: Bi<sub>2</sub>O<sub>3</sub> Monolayers from Elemental Liquid

### Bismuth

*Kibret A. Messalea<sup>a</sup>, Benjamin J. Carey<sup>b</sup>, Azmira Jannat<sup>a</sup>, Nitu Syed<sup>a</sup>, Md Mohiuddin<sup>a</sup>, Baoyue Zhang<sup>a</sup>, Ali Zavabeti<sup>a</sup>, Taimur Ahmed<sup>a</sup>, Nasir Mahmood<sup>a</sup>, Enrico Della Gaspera<sup>c</sup>, Khashayar Khoshmanesh<sup>a</sup>, Kourosh Kalantar-zadeh<sup>a,d</sup> and Torben Daeneke<sup>a</sup>*

a. School of Engineering, RMIT University, Melbourne, Victoria 3000, Australia

b. Institute of Physics and Center for Nanotechnology, University of Münster, 48149 Münster, Germany

c. School of Science, RMIT University, Melbourne, Victoria 3000, Australia

d. School of Chemical Engineering, University of New South Wales, Sydney 2052, New South Wales, Australia,

Correspondence to Torben Daeneke email: [torben.daeneke@rmit.edu.au](mailto:torben.daeneke@rmit.edu.au) or Kourosh Kalantar-zadeh email: [kourosh.kalantar@rmit.edu.au](mailto:kourosh.kalantar@rmit.edu.au)

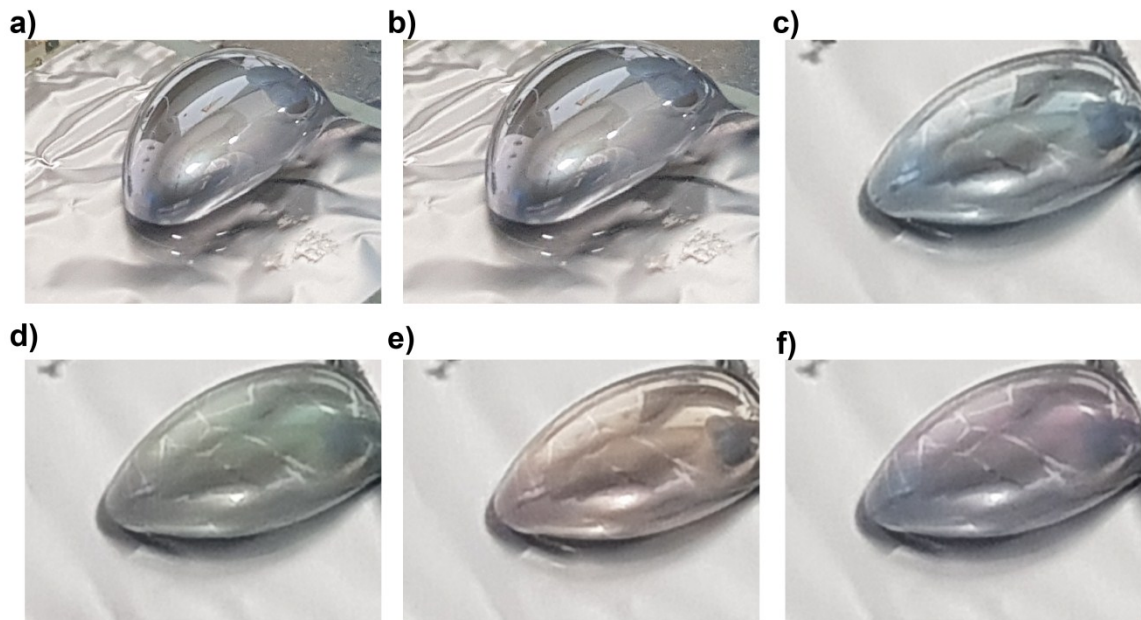


**Fig. S1** Oxidation stages of liquid bismuth in a flow through glove box which is continuously purged with nitrogen (oxygen level is 10-100 ppm) at ~300 °C a) Photograph directly after pre-conditioning. b) Photograph after 1 minute of oxidation. c) Photograph of liquid bismuth in an ambient air at~300 °C, directly after pre-conditioning. c&d) oxidation of liquid bismuth after 4&6 seconds in an ambient air f) oxidation of liquid bismuth after 1 minute in ambient air, featuring a thick oxide layer.

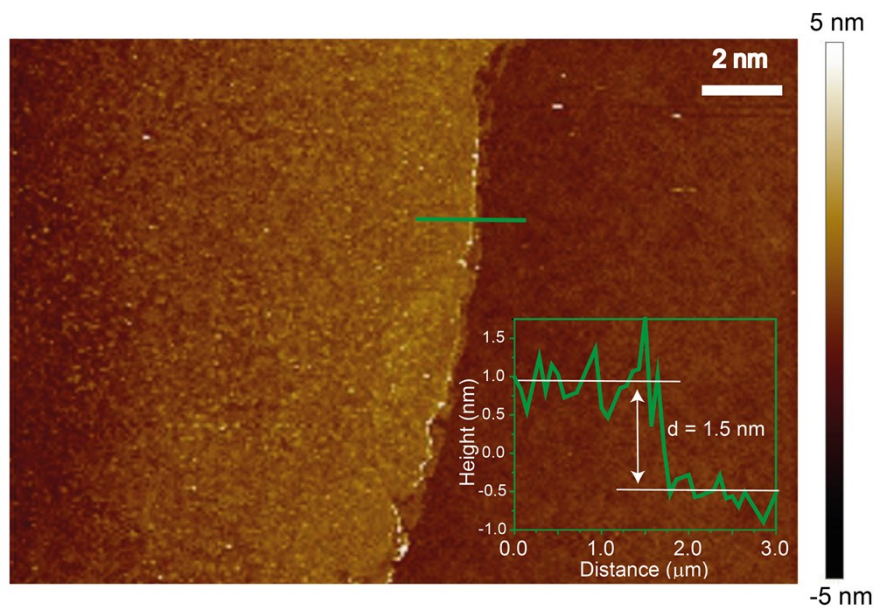


**Fig. S2** AFM Two atomic layers with folding edge synthesized in a in an ambient environment

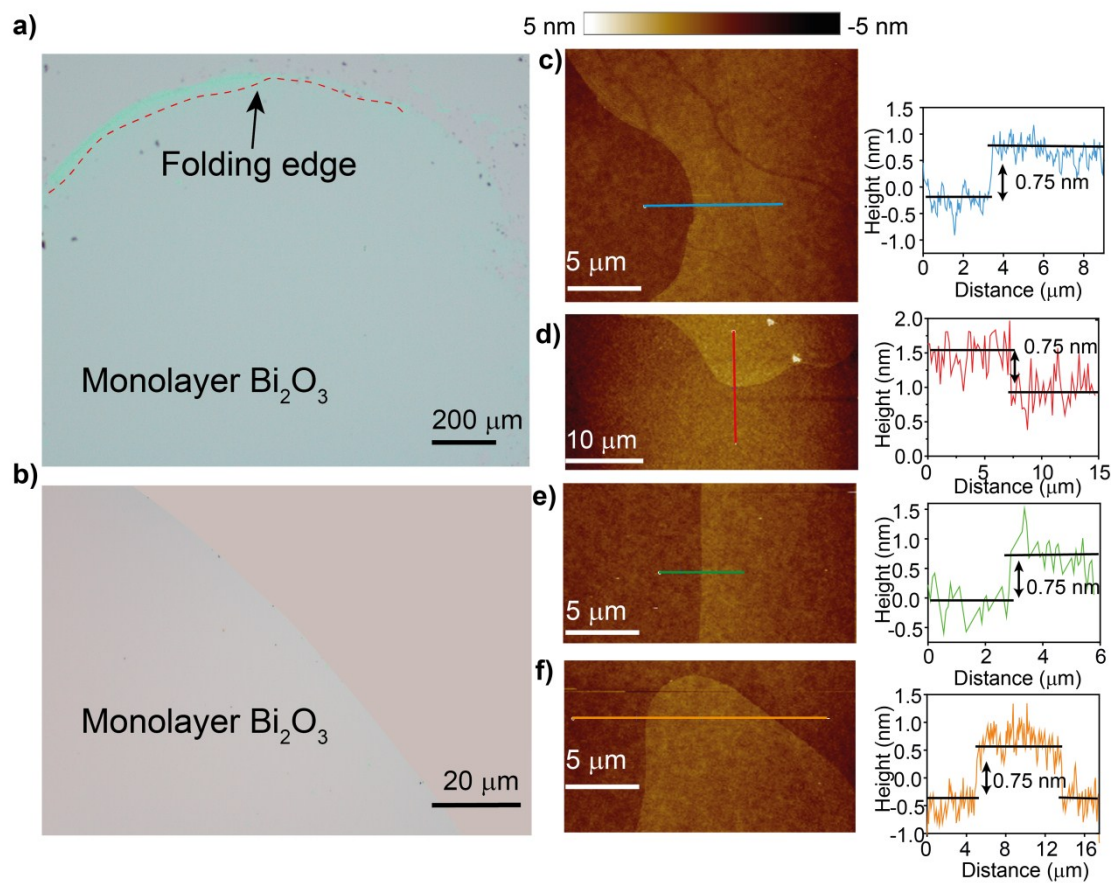


**Fig. S3** Morphology of the synthesised film a) optical image in millimetre scale showing large area monolayer  $\text{Bi}_2\text{O}_3$  with the pristine and homogeneous area and folding and cracking at the edge (red dotted line) of the monolayer b) optical image of monolayer in micrometre scale c-f) AFM image taken at four locations to show the monolayer edges and their corresponding profile plots.

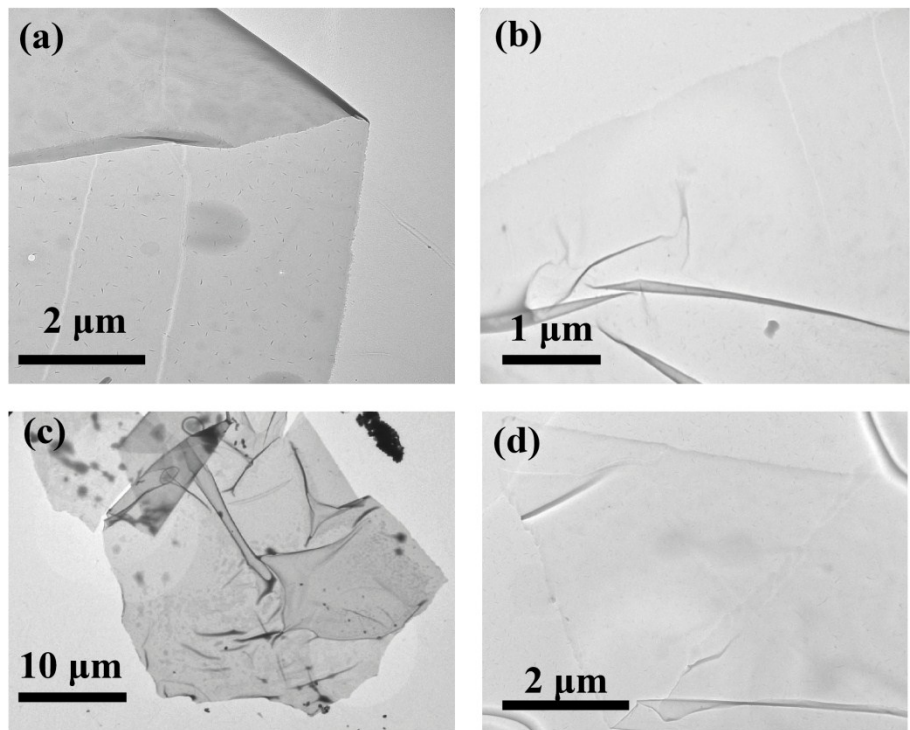


**Fig. S4** Additional TEM synthesised in oxygen controlled environment.

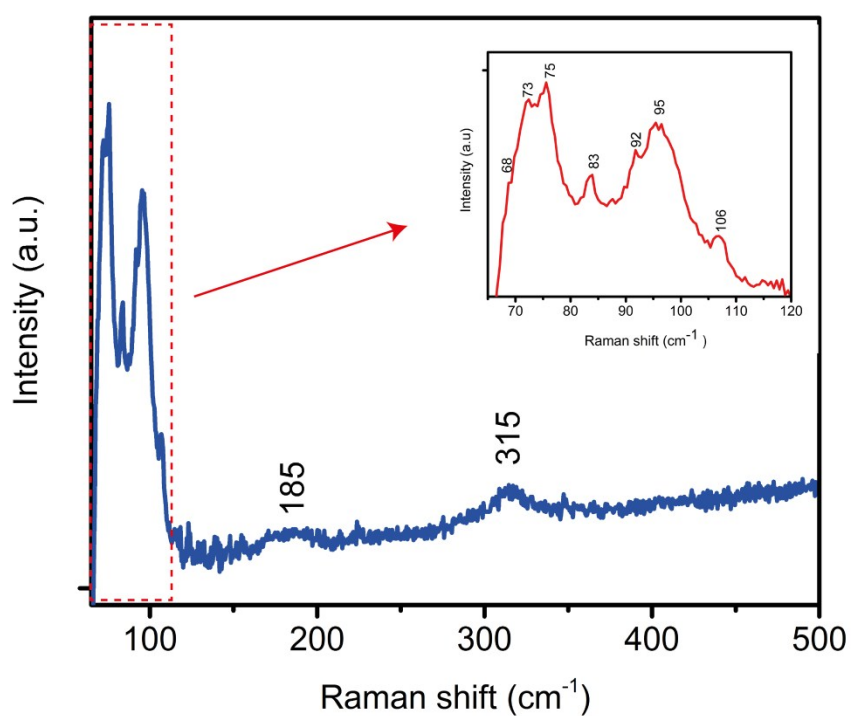


**Fig. S5** Extended Raman spectrum of ultrathin  $\alpha$ -Bi<sub>2</sub>O<sub>3</sub>

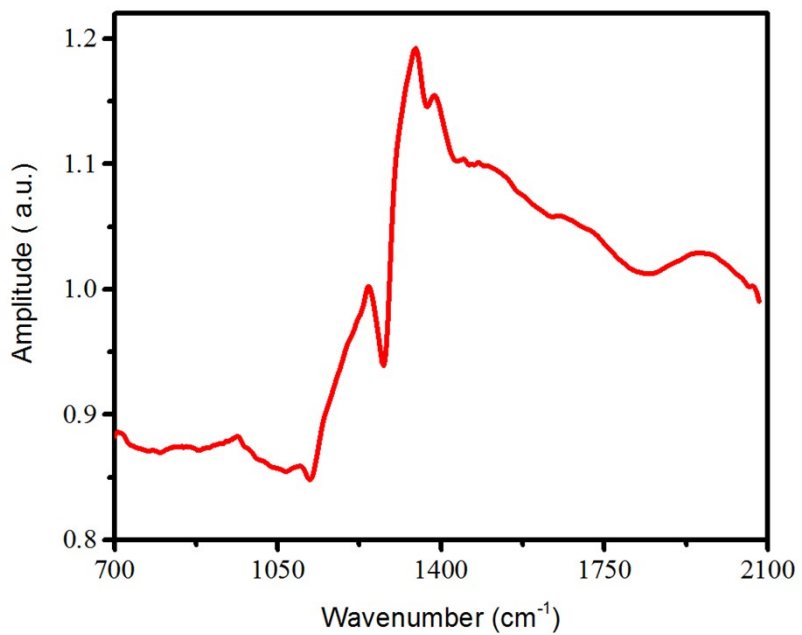


**Fig. S6** nano-FTIR of 2D  $\alpha$ - $\text{Bi}_2\text{O}_3$

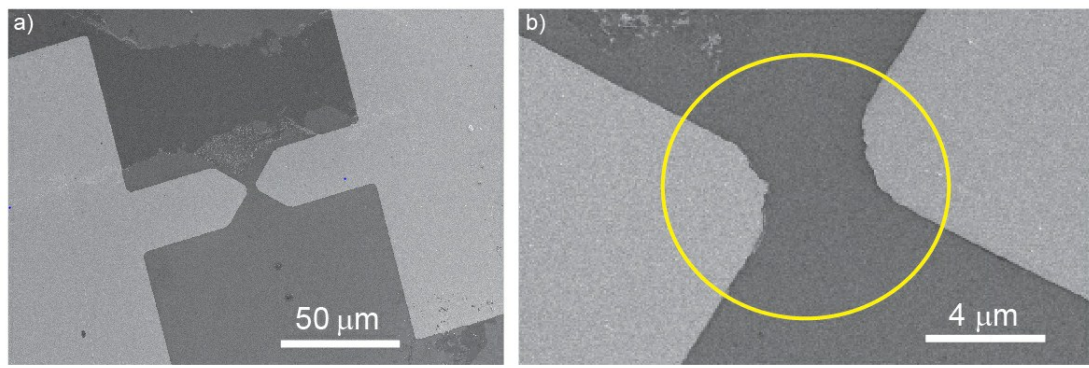


**Fig. S7** SEM image of photodetector device a) showing contrast between substrate and the nanosheets b) zoomed in view of contact electrodes deposited above the 2D nanosheets. The yellow circle shows the size of UV light spot that defines the area which is used in responsivity calculations and measurements.

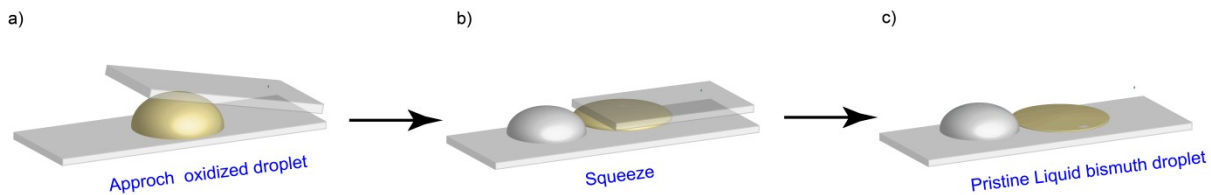


**Fig. S8** Schematic of the preconditioning process. a) Bismuth is melted on a clean glass slide inside a glove box. b) A second preheated glass slide is used to squeeze the liquid metal droplet. The process removes existing metal oxide residues which adhere to the glass substrates. c) A pristine molten metal droplet is obtained. The preheating of the second glass slide is performed to avoid the liquid metal from freezing. The process may be repeated multiple times in order to remove all re-existing oxides.

**Table S1** UV detectors based on 2D nano-materials

<b>Material</b>	<b>Spectral Range</b>	<b>Responsivity (AW<sup>-1</sup>)</b>	<b>Response time (ms)</b>	<b>Detectivity (Jones)</b>	<b>Ref.</b>
MoS <sub>2</sub>	UV-Visible-NIR	0.12	-	10 <sup>11</sup>	1
	UV-visible-NIR	3.6x10 <sup>-5</sup>	60	-	2
	UV-visible	6.3x10 <sup>-5</sup>	20	4.2x10 <sup>8</sup>	3
WS <sub>2</sub>	UV-visible-NIR	0.7	9.9x10 <sup>3</sup>	2.7x10 <sup>9</sup>	4
	UV-visible	53.3	-	1.22x10 <sup>11</sup>	5
GaS	UV-visible	19.2	<30	10 <sup>14</sup>	6
	UV-visible	2.8	20	-	7
GaSe	UV-visible	1.4	104	-	8
GaTe	UV-visible	274.4	48	10 <sup>12</sup>	9
	UV-visible	0.03	54	-	10
	UV-visible-NIR	3.95x10 <sup>-2</sup>	18	2.26x10 <sup>12</sup>	11
In <sub>2</sub> Se <sub>3</sub>	UV-visible-NIR	9.8x10 <sup>4</sup>	9x10 <sup>3</sup>	3.3x10 <sup>13</sup>	12
InSe	UV-visible-NIR	5.68x10 <sup>4</sup>	5	10 <sup>13</sup>	13
SnS <sub>2</sub>	UV-visible-NIR	1.05x10 <sup>-6</sup>	400	-	14
Bi <sub>2</sub> O <sub>3</sub>	UV-vis	400	0.07	1.1x10 <sup>13</sup>	This Work

**References:**

- W. Choi, M. Y. Cho, A. Konar, J. H. Lee, G. B. Cha, S. C. Hong, S. Kim, J. Kim, D. Jena, J. Joo and S. Kim, *Adv. Mater.*, 2012, **24**, 5832-5836.
- J. Li, M. M. Naiini, S. Vaziri, M. C. Lemme and M. Östling, *Adv. Func. Mater.*, 2014, **24**, 6524-6531.
- Y. Lee, J. Yang, D. Lee, Y. H. Kim, J. H. Park, H. Kim and J. H. Cho, *Nanoscale*, 2016, **8**, 9193-9200.
- J. D. Yao, Z. Q. Zheng, J. M. Shao and G. W. Yang, *Nanoscale*, 2015, **7**, 14974-14981.
- L. Zeng, L. Tao, C. Tang, B. Zhou, H. Long, Y. Chai, S. P. Lau and Y. H. Tsang, *Sci. Rep.*, 2016, **6**, 20343.

6. P. Hu, L. Wang, M. Yoon, J. Zhang, W. Feng, X. Wang, Z. Wen, J. C. Idrobo, Y. Miyamoto, D. B. Geohegan and K. Xiao, *Nano Lett.*, 2013, **13**, 1649-1654.
7. P. Hu, Z. Wen, L. Wang, P. Tan and K. Xiao, *ACS nano*, 2012, **6**, 5988-5994.
8. M. Mahjouri-Samani, R. Gresback, M. Tian, K. Wang, A. A. Puretzky, C. M. Rouleau, G. Eres, I. N. Ivanov, K. Xiao, M. A. McGuire, G. Duscher and D. B. Geohegan, *Adv. Func. Mater.*, 2014, **24**, 6365-6371.
9. P. Hu, J. Zhang, M. Yoon, X.-F. Qiao, X. Zhang, W. Feng, P. Tan, W. Zheng, J. Liu, X. Wang, J. C. Idrobo, D. B. Geohegan and K. Xiao, *Nano Res.*, 2014, **7**, 694-703.
10. Z. Wang, M. Safdar, M. Mirza, K. Xu, Q. Wang, Y. Huang, F. Wang, X. Zhan and J. He, *Nanoscale*, 2015, **7**, 7252-7258.
11. R. B. Jacobs-Gedrim, M. Shammugam, N. Jain, C. A. Durcan, M. T. Murphy, T. M. Murray, R. J. Matyi, R. L. Moore and B. Yu, *ACS nano*, 2013, **8**, 514-521.
12. J. O. Island, S. I. Blanter, M. Buscema, H. S. van der Zant and A. Castellanos-Gomez, *Nano Lett.*, 2015, **15**, 7853-7858.
13. W. Feng, J.-B. Wu, X. Li, W. Zheng, X. Zhou, K. Xiao, W. Cao, B. Yang, J.-C. Idrobo, L. Basile, W. Tian, P. Tan and P. Hu, *J. Mater. Chem. C*, 2015, **3**, 7022-7028.
14. Y. Tao, X. Wu, W. Wang and J. Wang, *J. Mater. Chem. C*, 2015, **3**, 1347-1353.